

Nucleosome occupancy landscape and dynamics at mouse recombination hotspots

Irina V. Getun¹, Zhen K. Wu¹, Ahmad M. Khalil² & Philippe R.J. Bois^{1*}

¹Genome Plasticity Laboratory, Department of Cancer Biology, The Scripps Research Institute, Scripps Florida, Jupiter, Florida, USA, and ²The Broad Institute of MIT and Harvard, Cambridge, Massachusetts, USA

During meiosis, paternal and maternal homologous chromosomes recombine at specific recombination sites named hotspots. What renders 2% of the mammalian genomes permissive to meiotic recombination by allowing Spo11 endonuclease to initiate double-strand breaks is largely unknown. Work in yeast has shown that chromatin accessibility seems to be important for this activity. Here, we define nucleosome profiles and dynamics at four mouse recombination hotspots by purifying highly enriched fractions of meiotic cells. We found that nucleosome occupancy is generally stable during meiosis progression. Interestingly, the cores of recombination hotspots have largely open chromatin structure, and the localization of the few nucleosomes present in these cores correlates precisely with the crossover-free zones in recombinogenic domains. Collectively, these high-resolution studies suggest that nucleosome occupancy seems to direct, at least in part, how meiotic recombination events are processed.

Keywords: epigenetics; meiosis; nucleosome; recombination; chromatin

EMBO reports (2010) 11, 555–560. doi:10.1038/embor.2010.79

INTRODUCTION

Meiotic recombination occurs at discrete regions in the genome, named hotspots. This process is triggered by double-strand breaks (DSBs) at these sites by the meiotic-specific endonuclease Spo11. Chromatin accessibility has long been suspected to have important roles in specifying the locale of hotspots, as supported by studies in yeast showing that these sites have an open chromatin structure (Wu & Lichten, 1994; Nicolas, 1998). Furthermore, some histone modifications affect the frequency and genome-wide patterns of meiotic recombination (Yamada *et al*, 2004; Mieczkowski *et al*, 2007; Merker *et al*, 2008; Borde *et al*, 2009). Thus, histones seem to have a role in rendering

chromatin permissive to Spo11-induced DSBs (Kniewel & Keeney, 2009); yet, how this occurs is not resolved.

The few direct epigenetic analyses reported so far in mammals are consistent with the idea that an open chromatin structure offers a 'site of opportunity' for directing meiotic recombination (Shenkar *et al*, 1991; Mizuno *et al*, 1996; Qin *et al*, 2004). Furthermore, recent studies on two highly recombinogenic hotspots suggest that a distinct histone code precedes DSB initiation, at least at these loci (Buard *et al*, 2009). However, the detailed analyses of mammalian recombination hotspots have been impaired by difficulties in purifying the entire spectrum of meiotic cells, from spermatogonia to diplotene cells, which include the leptotene–zygotene stage in which DSBs are generated.

To resolve this problem, we validated and developed further a fluorescence-activated cell sorting (FACS) methodology that allows one to simultaneously isolate the meiotic fractions from adult mice to more than 95% purity in a single experiment (Lassalle *et al*, 2004; Bastos *et al*, 2005). These cells were used to generate nucleosome occupancy maps by performing micrococcal nuclease (MNase) digestion combined with quantitative PCR oligo-tiling assays at four meiotic recombination hotspots on chromosome 19 (Litt *et al*, 2001; Lam *et al*, 2008). Three fundamental questions regarding the anatomy and control of mammalian meiotic recombination were addressed: Are nucleosome occupancy profiles stable during meiotic progression? Does nucleosome occupancy define distinct classes of hotspots? Does nucleosome positioning at hotspot cores directly influence crossover (CO) profiles? Our studies reveal that nucleosome occupancy landscapes at hotspots are stable and that their recombinogenic cores have a generally open chromatin structure. Interestingly, the few nucleosomes that are present at these cores precisely define CO repulsion zones where recombination does not occur. Thus, chromatin structure might affect, at least in part, the formation and resolution of recombinant molecules.

RESULTS

Purification of meiotic fractions

The mapping of nucleosome occupancy throughout meiosis requires a facile method to obtain highly purified fractions of all meiotic-stage cells. To this end, we refined and validated a FACS methodology using Hoechst stain, which allows one to efficiently

¹Genome Plasticity Laboratory, Department of Cancer Biology, The Scripps Research Institute, Scripps Florida, 130 Scripps Way #2C1, Jupiter, Florida 33458, USA

²The Broad Institute of MIT and Harvard, 7 Cambridge Center, Cambridge, Massachusetts 02142, USA

*Corresponding author. Tel: +1 561 228 3208; Fax: +1 561 288 3056;

E-mail: pbois@scripps.edu

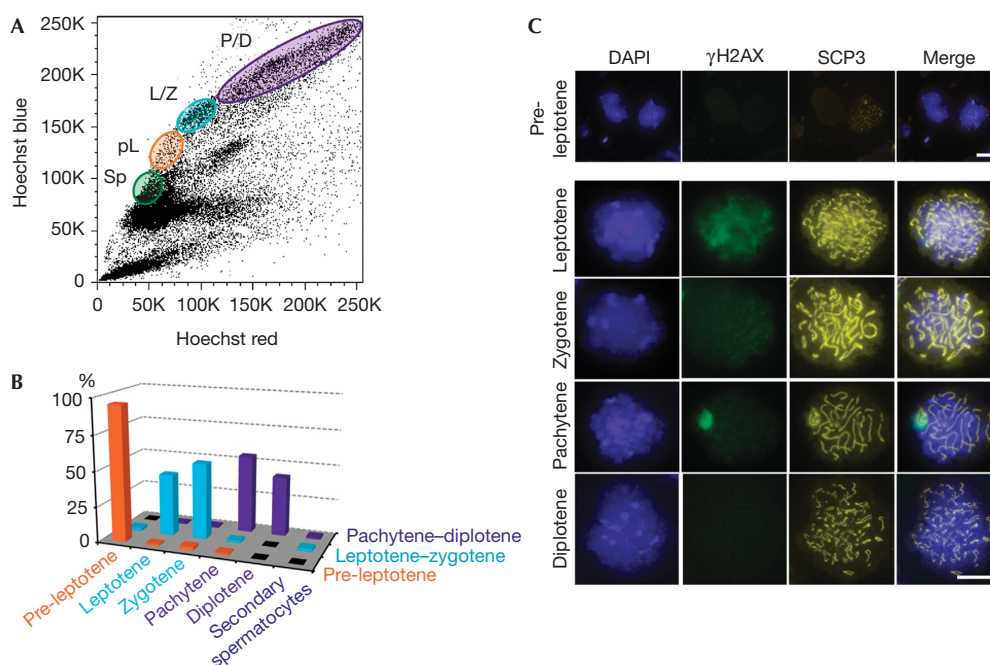


Fig 1 | Fluorescence-activated cell sorting purification and characterization of meiotic-stage cells from adult mice. (A) A representative Hoechst FACS profile, with the meiotic cell populations indicated. For this study, the four populations purified were spermatogonia (Sp), pre-leptotene (pL), leptotene-zygotene (L/Z) and pachytene-diplotene (P/D). (B) Graph indicating the percentage of each cell type per purified population: pre-leptotene (95%), leptotene-zygotene (43–53%) and pachytene-diplotene (42–55%). (C) Representative pictograms of meiotic cells of the purified fractions. Cells were counterstained with DAPI and co-immunostained with γ H2AX and SCP3 to confirm the stage of the FACS-sorted meiotic cell population. γ H2AX shows the diffuse staining before pachytene, where it becomes highly enriched on the XY-sex body. SCP3 becomes clearly visible at leptotene and zygotene, and at pachytene it forms perfectly along the length of the homologous chromosomes, but then it begins to disintegrate at diplotene. Scale bars, 20 μ m. DAPI, 4,6-diamidino-2-phenylindole; γ H2AX, phosphorylated histone H2AX; FACS, fluorescence-activated cell sorting; SCP3, synaptonemal complex protein 3.

purify various meiotic fractions from testicular cells dissociated from adult male mice, and thus obtained robust and reliable FACS profiles (Fig 1; Romrell *et al*, 1976; Lassalle *et al*, 2004; Bastos *et al*, 2005). To limit the experimental variation, we used a method by which all the main meiotic fractions from adult mice can be purified at once. The correct stage and level of purity of these sorted fractions, including pre-leptotene, leptotene-zygotene and pachytene-diplotene, were confirmed by immunofluorescence analyses using antibodies against the stage-specific meiosis markers, phosphorylated histone H2AX and the synaptonemal complex protein 3 (Fig 1; supplementary Fig S1 online). These analyses established that the sorted fractions were highly enriched, with more than 95% purity for pre-leptotene, leptotene-zygotene and pachytene-diplotene cells. Importantly, the minor contaminating cells in each fraction were strictly due to adjacent fractions of meiotic cells. By using this approach, 0.5–2.0 million cells of each meiotic fraction were isolated per sort (supplementary methods online).

Meiotic nucleosome landscape and dynamics

To define the local structure of chromatin surrounding the meiotic recombination hotspots, we used a well-defined method of native (non-crosslinked) chromatin digestion by MNase, which allows one to achieve high-resolution nucleosome mapping (Hebbes *et al*, 1994; Litt *et al*, 2001; Kharchenko *et al*, 2008; Schones *et al*,

2008). This technique generates mostly mono-nucleosomal DNA, which was analysed by quantitative PCR using SYBR green detection (see Methods; Fig 2A; supplementary methods online). To identify nucleosome positions, we used primer pair tiling across the selected loci, using 80–100 bp amplicons that overlap by 30–50 bp (Fig 2), a method similar to that used previously for mapping yeast promoters (Lam *et al*, 2008). Here, amplification of primer pairs, following MNase digestion equivalent to undigested input DNA, indicates the presence of a protecting mono-nucleosome, while the absence of amplification signifies a region of open chromatin susceptible to MNase digestion. Nucleosome positions are determined by calculating the fold change between MNase-treated samples and the undigested genomic DNA at an equivalent input (see Methods). We validated that nucleosomes were at the origin of these peaks by using a series of controls. First, we demonstrated that no MNase-resistant fragments were present at the four hotspots by using naked DNA (supplementary Fig S2 online). Second, we performed histone H3 chromatin immunoprecipitation on meiotic cells after crosslinking and sonication (supplementary Fig S3 online). This demonstrated that recombination hotspots were enriched selectively in chromatin immunoprecipitated with the H3 antibody but not in the case of no antibody control. Finally, because of the reduced resolution owing to sonication and using our oligo-tiling detection strategy, we performed native chromatin immunoprecipitation with histone

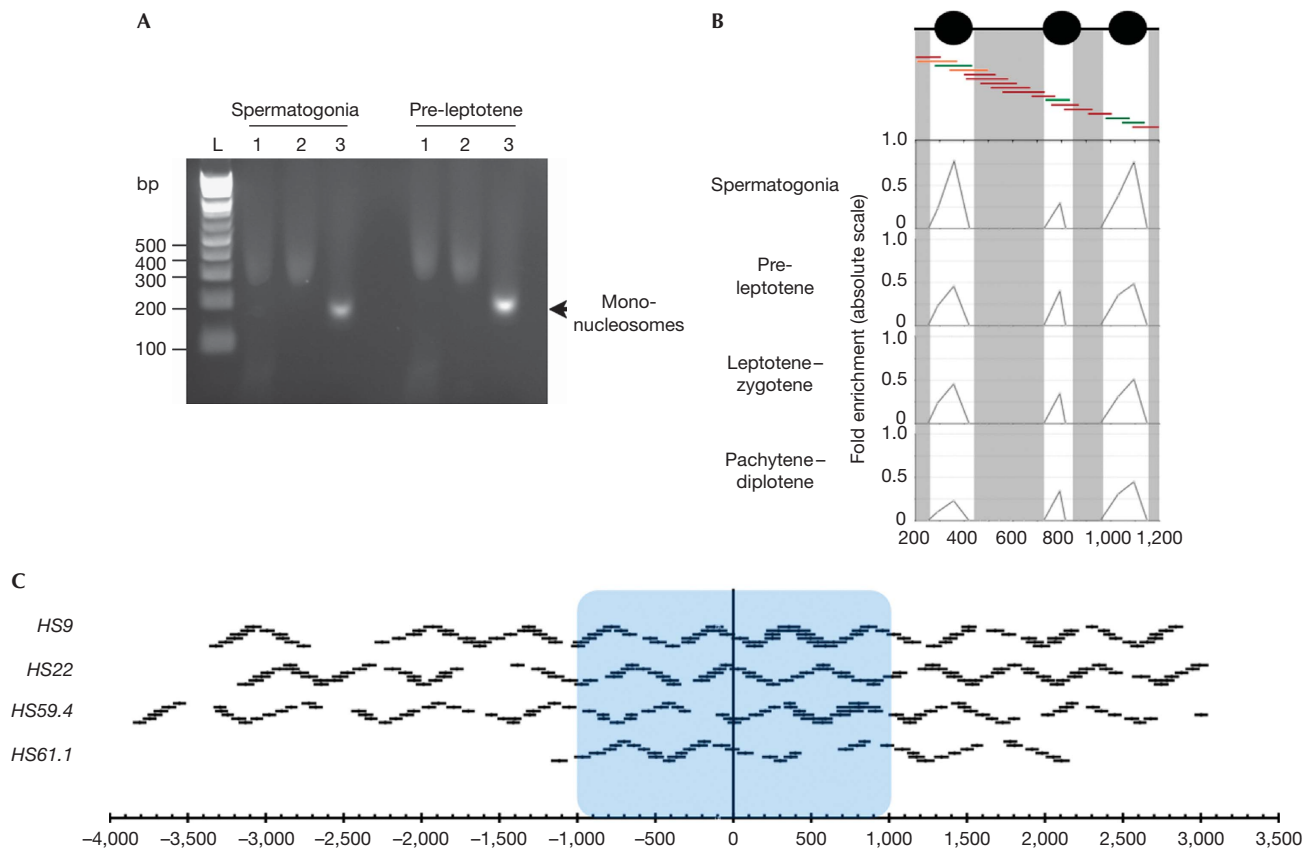


Fig 2 | Schematic of the nucleosome mapping technique. (A) Typical mono-nucleosome preparation from the indicated FACS-purified meiotic cells is shown. Lanes 1 correspond to the total chromatin fraction after MNase digestion, lanes 2 indicate the extracted nucleosomes after native chromatin treatment and lanes 3 show the purified mono-nucleosomes after desalting. The high salt concentration causes aberrant migration in lanes 1 and 2. (B) FACS-purified meiotic fractions are digested to completion with MNase, DNA is purified and mono-nucleosome fragments are isolated. Mono-nucleosomal DNA is used as a template for quantitative PCR with overlapping primer pairs. A small 1 kb region is shown at the *HS9* locus. Protection of DNA from MNase digestion by nucleosomes will result in a robust PCR signal (green primer pairs), partial protection in an intermediate PCR signal (orange) and no protection in a trace PCR signal (dark red). Profiles are shown at the four studied stages as indicated. (C) Diagram representing all the primer pairs used for the four studied hotspots. The blue box indicates the approximate recombinogenic core. Gaps in the oligonucleotide pairs were owing to simple repeats, poor efficiency or primer pair failure to yield unique products. FACS, fluorescence-activated cell sorting; MNase, micrococcal nuclease.

H3 antibody on the MNase-treated fractions (supplementary Fig S4 online). These analyses confirmed that the MNase profiles correspond to locales of nucleosomes rather than other chromatin-binding factors, which require crosslinking to be identified.

By using these approaches, the nucleosome landscape at the four recombination hotspots (*HS9*, *HS22*, *HS59.4* and *HS61.1*) of mouse chromosome 19 was defined throughout meiosis. Globally stable and highly reproducible profiles were observed, with all meiotic fractions showing virtually identical landscapes at each of the four hotspots (Fig 3). Thus, it seems that the overall local chromatin landscape of these hotspots is established before the initiation of meiosis and that it is not overtly reorganized during meiotic progression. This suggests that chromatin structure is defined primarily by the intrinsic DNA sequence preferences of nucleosomes, as shown in yeast (Kaplan *et al*, 2009). This was confirmed by applying the same approach to primary somatic thymic cells, for which the nucleosome occupancy landscapes at the four hotspots were nearly identical to those present in

meiotic cells, suggesting that gross chromatin remodelling is not operational at hotspots during meiosis (Fig 3).

Nucleosome profiling established that the cores of these hotspots were generally open, with 300–1,000 bp nucleosome-free domains (Fig 3), reminiscent of those found at yeast recombination hotspots (Ohta *et al*, 1994; Wu & Lichten, 1994). Interestingly, three out of the four hotspot cores were not nucleosome-free. First, the cores were flanked immediately by histones. Second, two similar profiles were observed with *HS9* and *HS61.1*, with no or only one nucleosome on the telomeric (right) side of the recombinogenic core (Fig 3), respectively. By contrast, the cores of the *HS22* and *HS59.4* hotspots have nucleosomes at the very centre of the permissive region that are flanked by open chromatin. Specifically, *HS22* harbours two central nucleosomes surrounded on each side by 700 bp of open chromatin, whereas *HS59.4* had one central nucleosome flanked by 700 bp (centromeric, left) and 1,000 bp (telomeric, right) of nucleosome-free chromatin (Fig 3).

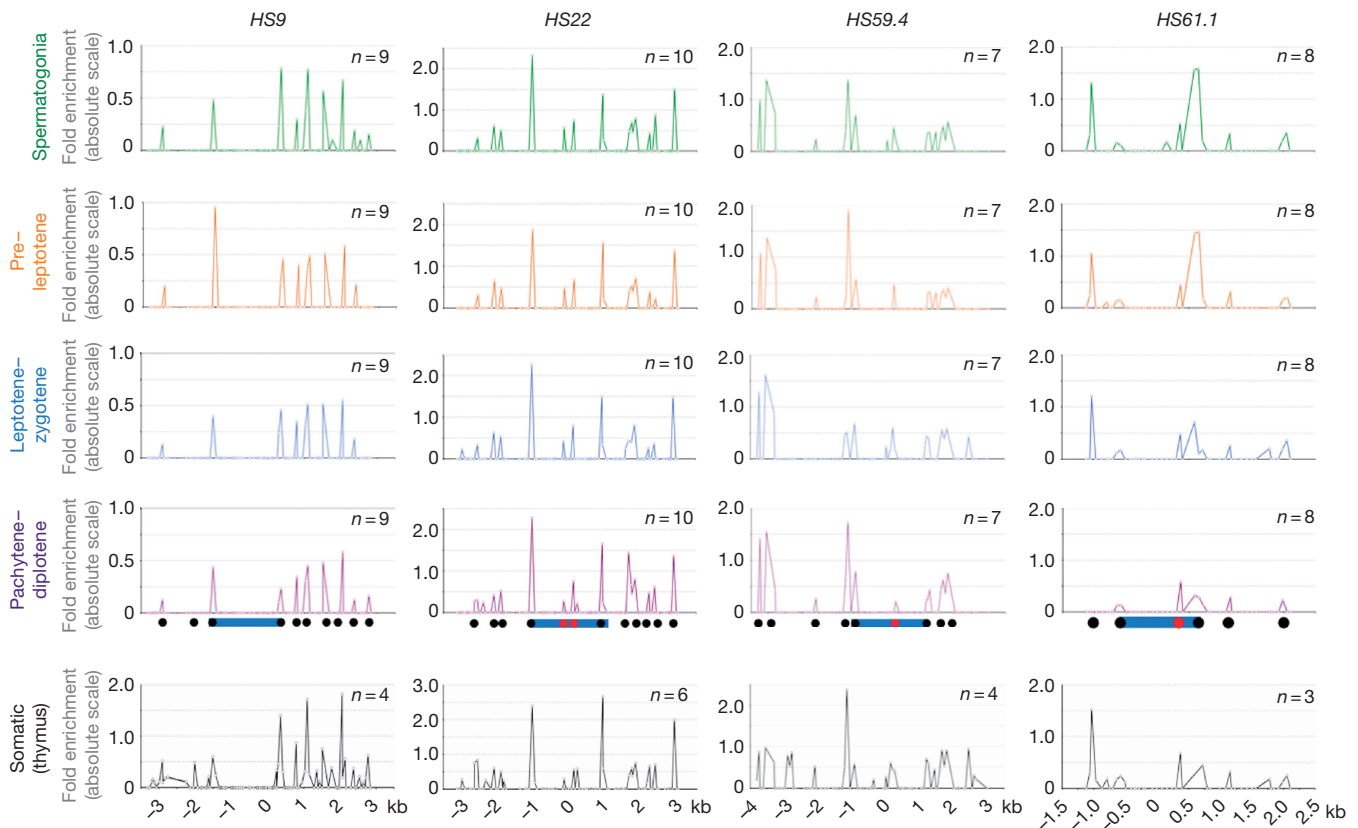


Fig 3 | Nucleosome occupancy at the four meiotic hotspots during meiotic progression. Nucleosome profiles at the recombination hotspots in spermatogonia, pre-leptotene, leptotene–zygotene and pachytene–diplotene meiotic fractions, as well as in somatic primary thymic cells, are shown for each of the indicated hotspots. Profiles are absolute, with the vertical scale being the fold enrichment between the mono-nucleosome MNase-digested DNA fraction and undigested genomic DNA, which is calculated by using the formula $2^{-\Delta Ct}$. The x-axis represents the location across the analysed locus. Nucleosome positions outside (black) or within (red) hotspot cores (blue) are indicated. The numbers of independent experimental repeats for each profile are shown. MNase, micrococcal nuclease.

The overall open chromatin architecture, however, was not restricted to hotspot cores, suggesting that open chromatin might be necessary, but not sufficient, to confer recombinogenicity. Indeed, the coverage of the nucleosome occupancy maps at *HS9*, *HS22* and *HS59.4* was 6.5, 6.0 and 7.0 kb, respectively, which is well above the 1.5–2.5 kb of the recombination hotspot cores; thus, recombinationally cold regions can also have large nucleosome-free domains (Fig 3). Further analysis covering 1 kb at the –25, –10, +10 and +25 kb regions surrounding the cores of these hotspots confirmed this feature, with most of these domains containing open chromatin (supplementary Fig S5 online). Thus, although open chromatin is present at the cores of recombination hotspots, this is not sufficient to define sites of DSB opportunity.

Nucleosome location defines CO repulsion zones

The detailed CO profiles of the *HS22*, *HS59.4* and *HS61.1* loci identified domains refractory for CO resolution (Fig 4). These refractory zones have also been observed at human hotspots such as *MSNID* and *MSTN1a/b* (Jeffreys & Neumann, 2005; Neumann & Jeffreys, 2006). These regions appear to be randomly positioned across the hotspots, wherein CO refractory zones are near the centre of the *HS22* and *HS59.4* hotspot cores, compared with at

the 3′-boundary of the *HS61.1* hotspot core (black arrows, Fig 4; supplementary Figs S6,S7 online). Importantly, superposing the nucleosome occupancy maps of these three loci with the CO profiles revealed that, in all the three hotspots, nucleosomes are located precisely at the sites that are excluded from CO resolution. These findings suggest roles for nucleosomes in directing CO resolution, perhaps by affecting strand invasion and D-loop extension (Wu et al, 2010).

DISCUSSION

This study provides, for the first time—to the best of our knowledge—detailed and high-resolution maps of nucleosome occupancy landscapes at mammalian recombination hotspots. Our analyses suggest that, like in yeast, chromatin organization seems to influence, at least in part, the process of meiotic recombination. First, our findings establish that nucleosome profiles are not meiosis-specific and that no major chromatin remodelling occurs to direct DSB initiation. Indeed, as the intrinsic sequence preference of nucleosomes is the main factor that determines their organization *in vivo* (Kaplan et al, 2009), this suggests that, unlike transcription factor binding sites or transcription start sites, no meiotic-specific factors remodel recombination

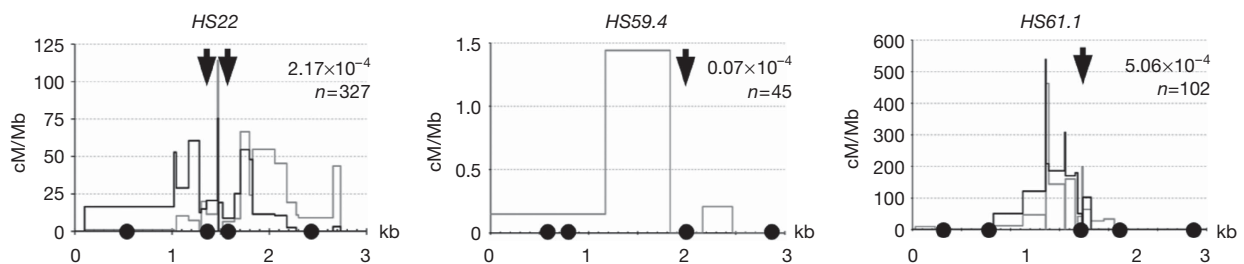


Fig 4 | Nucleosome positioning within the hotspot core is correlated with the crossover repulsion zones. Recombination profiles of *HS22*, *HS59.4* and *HS61.1* are shown. Both CO orientations are shown with B6-to-DBA (black) and DBA-to-B6 (grey); only the latter orientation is shown for *HS59.4*. Recombination rates and the number of molecules analysed to obtain the CO profiles at each hotspot are indicated. Nucleosomes are drawn to scale. Black arrows indicate the CO refractory zones within the hotspot cores (Wu *et al*, 2010). CO, crossover.

hotspots. However, it is possible that further factors such as competition between histone variants, effects of nucleosome modifications and higher-order folding of chromatin might participate in the deposition and landscape of nucleosomes. Our findings are similar to those in yeast, in which the MNase hypersensitivity at DSB sites following meiosis induction is suppressed or induced in parallel with DSBs themselves, without changes in the positioning of nucleosomes (Ohta *et al*, 1999). What triggers the initiation of meiotic recombination directly is a matter of considerable debate; yet, recent studies in yeast and mouse have suggested some of the controls that might have a role. For example, a potential histone code has been invoked in this response, in particular trimethylation of Lys 4 of histone H3 (Borde *et al*, 2009; Buard *et al*, 2009). However, it is not clear whether this mark is truly instructive or is simply a bystander effect, as this mark exists before the induction of meiosis in yeast (Borde *et al*, 2009).

Another important finding is that the hotspot core profiles show relatively similar structures with flanking nucleosomes (1.6–2.2 kb apart) and few within the core, establishing that the Spo11 complex is permissive to similar nucleosome environments. First, the observed core width is in excellent agreement with the CO profiles (1.5–2.5 kb) observed in the numerous hotspots analysed directly in mice and humans (Bois, 2007; Webb *et al*, 2008; Wu *et al*, 2010). Such a landscape would indicate a universal ‘footprint’ similar to what has been observed in eukaryotic promoters with nucleosome depletion at the transcription start sites (Ioshikhes *et al*, 2006). However, whereas biased DNA content is observed in the latter case, more global analysis will be necessary for mammalian hotspots. The present bottleneck resides in obtaining a sub-kb genome map of recombination hotspots. Second, the presence of nucleosomes at the centre of the hotspots is also consistent with a recent histone modification analysis performed at a lower resolution for the *Psmb9* and *Hlx1* hotspots (Buard *et al*, 2009). It is tempting to speculate that these nucleosomes might function as anchors for the Spo11 complex, at least for the sites that lie in the middle of the core (that is, *HS22* and *HS59.4*). Again, whether these hotspot core nucleosomes have passive or active roles in DSB initiation remains to be resolved.

Importantly, our finding that CO repulsion zones are correlated with sites of nucleosome occupancy suggests that local chromatin influences the mechanism of homologous repair. Indeed, two combined mechanisms could explain the correlation between CO repulsion zones and the nucleosome landscape. First, local

nucleosome occupancy could directly affect the site selection of DSBs by Spo11. Indeed, biochemical studies using reconstituted chromatin have shown that nucleosomes are a physical barrier for the cleavage activity of DNA topoisomerases *in vivo* (Di Felice *et al*, 2008). In this background, DSBs can only occur in open chromatin domains with the direct consequence of favouring single-strand capture on the homologous open regions. Second, D-loop formation on the homologue chromosome and the subsequent synthesis-dependent strand annealing extension, second strand capture and double Holliday junction (dHJ) formation will be favoured towards open chromatin (McMahill *et al*, 2007). By contrast, nucleosomes will constrain D-loop formation during synthesis-dependent strand annealing and thus promote non-CO resolution. Finally, flanking nucleosomes would harness runaway sliding of dHJs. Collectively, our observations support a model in which local chromatin organization might have a fundamental but passive role in directing DSB initiation and subsequent D-loop stabilization in nucleosome-free domains, but might have direct consequences for DSB initiation, dHJ formation and choice of CO/non-CO resolution (Wu *et al*, 2010).

Our analyses provide the initial snapshots of the nucleosome landscapes at mammalian meiotic recombination hotspots and their effect on CO resolution profiles. They also reveal that generating a DSB initiation site requires additional layers of control that still need to be defined. The methods developed and validated in this study, which allow one to obtain simultaneously highly purified pre- and post-DSB meiotic cells, provide the necessary platform for studies that could ultimately define the features and regulatory mechanisms that render a genomic location permissive to DSB initiation.

METHODS

Mouse strains. The mice used in this study were bred and maintained at the Animal Resource Center facility of The Scripps Research Institute, Scripps Florida, following the guidelines of the Institutional Animal Care and Use Committee and an approved animal protocol. C57Bl/6J, DBA/2J and C57Bl/6J × DBA/2J F1 (female C57Bl/6J × male DBA/2J) mice were obtained from the Jackson Laboratory. In house, B6xDBA hybrids were also generated. Mice used for this study were at least 10 weeks of age. **Testis cell dissociation and FACS enrichment and immunocytochemistry.** Spermatogonia, pre-leptotene, leptotene–zygotene and pachytene–diplotene cell fractions were purified using the previously described FACS-based methodology (Lassalle *et al*,

2004; Bastos *et al*, 2005). Cell dissociation is crucial for this method and therefore we adapted a previously described protocol (Romrell *et al*, 1976). Detailed protocols are provided in the supplementary methods online.

MNase digestion and nucleosome profiles. Mono-nucleosomes were isolated from native chromatin of either meiotic or somatic C57Bl/6J × DBA/2J F1 mouse cells as described (Hebbes *et al*, 1994; Litt *et al*, 2001). In all, 0.5 to 2 × 10⁶ FACS-sorted cells were lysed to obtain nuclei, which were divided into four equal aliquots and digested with increasing amounts of MNase. The MNase reactions were performed for 10 min at 37 °C and stopped by adding ethylenediaminetetraacetic acid to a final concentration of 10 mM. The digests were combined and mono-nucleosomes were isolated and purified. Finally, DNA from purified nucleosomal fractions was isolated, quantified and used for real-time PCR analysis. Primers used for quantitative real-time PCR are listed in supplementary Tables S1–S7 online. The nucleosomal occupancy level for a given DNA region surveyed was calculated by using the formula 2^{-ΔCt}, in which ΔCt = MNase-digested DNA Ct – the input undigested DNA Ct. Detailed protocols are provided in the supplementary methods online.

Supplementary information is available at *EMBO reports* online (<http://www.emboreports.org>).

ACKNOWLEDGEMENTS

We are indebted to Drs J. Cleveland and T. Izard for their critical comments regarding the paper, to Dr H. Petrie, B. Anderson and B. Torres (Scripps Florida FACS core) for their crucial technical advice and assistance, and to numerous colleagues and reviewers for their discussions and insights. This paper is dedicated to our friend Mark Hall. This project was supported in part by funding from the State of Florida to Scripps and award number R01GM085079 from the National Institute of General Medical Sciences. This is manuscript number 19906 of The Scripps Research Institute.

CONFLICT OF INTEREST

The authors declare that they have no conflict of interest.

REFERENCES

- Bastos H, Lassalle B, Chicheportiche A, Riou L, Testart J, Allemand I, Fouchet P (2005) Flow cytometric characterization of viable meiotic and postmeiotic cells by Hoechst 33342 in mouse spermatogenesis. *Cytometry A* **65**: 40–49
- Bois PR (2007) A highly polymorphic meiotic recombination mouse hotspot exhibits incomplete repair. *Mol Cell Biol* **27**: 7053–7062
- Borde V, Robine N, Lin W, Bonfils S, Geli V, Nicolas A (2009) Histone H3 lysine 4 trimethylation marks meiotic recombination initiation sites. *EMBO J* **28**: 99–111
- Buard J, Barthes P, Grey C, de Massy B (2009) Distinct histone modifications define initiation and repair of meiotic recombination in the mouse. *EMBO J* **28**: 2616–2624
- Di Felice F, Chiani F, Camilloni G (2008) Nucleosomes represent a physical barrier for cleavage activity of DNA topoisomerase I *in vivo*. *Biochem J* **409**: 651–656
- Hebbes TR, Clayton AL, Thorne AW, Crane-Robinson C (1994) Core histone hyperacetylation co-maps with generalized DNase I sensitivity in the chicken β-globin chromosomal domain. *EMBO J* **13**: 1823–1830
- Ioshikhes IP, Albert I, Zanton SJ, Pugh BF (2006) Nucleosome positions predicted through comparative genomics. *Nat Genet* **38**: 1210–1215
- Jeffreys AJ, Neumann R (2005) Factors influencing recombination frequency and distribution in a human meiotic crossover hotspot. *Hum Mol Genet* **14**: 2277–2287
- Kaplan N *et al* (2009) The DNA-encoded nucleosome organization of a eukaryotic genome. *Nature* **458**: 362–366
- Kharchenko PV, Woo CJ, Tolstorukov MY, Kingston RE, Park PJ (2008) Nucleosome positioning in human HOX gene clusters. *Genome Res* **18**: 1554–1561
- Kniewel R, Keeney S (2009) Histone methylation sets the stage for meiotic DNA breaks. *EMBO J* **28**: 81–83
- Lam FH, Steger DJ, O’Shea EK (2008) Chromatin decouples promoter threshold from dynamic range. *Nature* **453**: 246–250
- Lassalle B, Bastos H, Louis JP, Riou L, Testart J, Dutrillaux B, Fouchet P, Allemand I (2004) ‘Side Population’ cells in adult mouse testis express *Bcrp1* gene and are enriched in spermatogonia and germinal stem cells. *Development* **131**: 479–487
- Litt MD, Simpson M, Recillas-Targa F, Prioleau MN, Felsenfeld G (2001) Transitions in histone acetylation reveal boundaries of three separately regulated neighboring loci. *EMBO J* **20**: 2224–2235
- McMahill MS, Sham CW, Bishop DK (2007) Synthesis-dependent strand annealing in meiosis. *PLoS Biol* **5**: e299
- Merker JD, Dominska M, Greenwell PW, Rinella E, Bouck DC, Shibata Y, Strahl BD, Mieczkowski P, Petes TD (2008) The histone methylase Set2p and the histone deacetylase Rpd3p repress meiotic recombination at the HIS4 meiotic recombination hotspot in *Saccharomyces cerevisiae*. *DNA Repair* **7**: 1298–1308
- Mieczkowski PA, Dominska M, Buck MJ, Lieb JD, Petes TD (2007) Loss of a histone deacetylase dramatically alters the genomic distribution of Spo11p-catalyzed DNA breaks in *Saccharomyces cerevisiae*. *Proc Natl Acad Sci USA* **104**: 3955–3960
- Mizuno K, Koide T, Sagai T, Moriwaki K, Shiroishi T (1996) Molecular analysis of a recombinational hotspot adjacent to *Lmp2* gene in the mouse MHC: fine location and chromatin structure. *Mamm Genome* **7**: 490–496
- Neumann R, Jeffreys AJ (2006) Polymorphism in the activity of human crossover hotspots independent of local DNA sequence variation. *Hum Mol Genet* **15**: 1401–1411
- Nicolas A (1998) Relationship between transcription and initiation of meiotic recombination: toward chromatin accessibility. *Proc Natl Acad Sci USA* **95**: 87–89
- Ohta K, Shibata T, Nicolas A (1994) Changes in chromatin structure at recombination initiation sites during yeast meiosis. *EMBO J* **13**: 5754–5763
- Ohta K, Wu TC, Lichten M, Shibata T (1999) Competitive inactivation of a double-strand DNA break site involves parallel suppression of meiosis-induced changes in chromatin configuration. *Nucl Acids Res* **27**: 2175–2180
- Qin J, Richardson LL, Jasin M, Handel MA, Arnheim N (2004) Mouse strains with an active H2-Ea meiotic recombination hot spot exhibit increased levels of H2-Ea-specific DNA breaks in testicular germ cells. *Mol Cell Biol* **24**: 1655–1666
- Romrell LJ, Bellve AR, Fawcett DW (1976) Separation of mouse spermatogenic cells by sedimentation velocity. A morphological characterization. *Dev Biol* **49**: 119–131
- Schones DE, Cui K, Cuddapah S, Roh TY, Barski A, Wang Z, Wei G, Zhao K (2008) Dynamic regulation of nucleosome positioning in the human genome. *Cell* **132**: 887–898
- Shenkar R, Shen MH, Arnheim N (1991) DNase I-hypersensitive sites and transcription factor-binding motifs within the mouse E beta meiotic recombination hot spot. *Mol Cell Biol* **11**: 1813–1819
- Webb AJ, Berg IL, Jeffreys A (2008) Sperm cross-over activity in regions of the human genome showing extreme breakdown of marker association. *Proc Natl Acad Sci USA* **105**: 10471–10476
- Wu TC, Lichten M (1994) Meiosis-induced double-strand break sites determined by yeast chromatin structure. *Science* **263**: 515–518
- Wu ZK, Getun IV, Bois PR (2010) Anatomy of mouse recombination hot spots. *Nucl Acids Res* **38**: 2346–2354
- Yamada T, Mizuno K, Hirota K, Kon N, Wahls WP, Hartsuiker E, Murofushi H, Shibata T, Ohta K (2004) Roles of histone acetylation and chromatin remodeling factor in a meiotic recombination hotspot. *EMBO J* **23**: 1792–1803